

Search for Charmonium States Decaying to $J/\psi\gamma\gamma$ Using Initial-State Radiation Events

The BABAR Collaboration

February 7, 2008

Abstract

We study the processes $e^+e^- \rightarrow (J/\psi\gamma\gamma)\gamma$ and $e^+e^- \rightarrow (J/\psi\pi^-\pi^+)\gamma$ where the hard photon radiated from an initial e^+e^- collision with center-of-mass (CM) energy near 10.58 GeV is detected. In the final state $J/\psi\gamma\gamma$ we consider $J/\psi\pi^0$, $J/\psi\eta$, $\chi_{c1}\gamma$, and $\chi_{c2}\gamma$ candidates. The invariant mass of the hadronic final state defines the effective e^+e^- CM energy in each event, so these data can be compared with direct e^+e^- measurements. We report 90% CL upper limits for the integrated cross section times branching fractions of the $J/\psi\gamma\gamma$ channels in the $Y(4260)$ mass region.

Submitted to the 33rd International Conference on High-Energy Physics, ICHEP 06,
26 July—2 August 2006, Moscow, Russia.

Stanford Linear Accelerator Center, Stanford University, Stanford, CA 94309

Work supported in part by Department of Energy contract DE-AC03-76SF00515.

The BABAR Collaboration,

B. Aubert, R. Barate, M. Bona, D. Boutigny, F. Couderc, Y. Karyotakis, J. P. Lees, V. Poireau,
V. Tisserand, A. Zghiche

*Laboratoire de Physique des Particules, IN2P3/CNRS et Université de Savoie, F-74941 Annecy-Le-Vieux,
France*

E. Grauges

Universitat de Barcelona, Facultat de Física, Departament ECM, E-08028 Barcelona, Spain

A. Palano

Università di Bari, Dipartimento di Fisica and INFN, I-70126 Bari, Italy

J. C. Chen, N. D. Qi, G. Rong, P. Wang, Y. S. Zhu

Institute of High Energy Physics, Beijing 100039, China

G. Eigen, I. Ofte, B. Stugu

University of Bergen, Institute of Physics, N-5007 Bergen, Norway

G. S. Abrams, M. Battaglia, D. N. Brown, J. Button-Shafer, R. N. Cahn, E. Charles, M. S. Gill,
Y. Groyzman, R. G. Jacobsen, J. A. Kadyk, L. T. Kerth, Yu. G. Kolomensky, G. Kukartsev, G. Lynch,
L. M. Mir, T. J. Orimoto, M. Pripstein, N. A. Roe, M. T. Ronan, W. A. Wenzel

Lawrence Berkeley National Laboratory and University of California, Berkeley, California 94720, USA

P. del Amo Sanchez, M. Barrett, K. E. Ford, A. J. Hart, T. J. Harrison, C. M. Hawkes, S. E. Morgan,
A. T. Watson

University of Birmingham, Birmingham, B15 2TT, United Kingdom

T. Held, H. Koch, B. Lewandowski, M. Pelizaeus, K. Peters, T. Schroeder, M. Steinke

Ruhr Universität Bochum, Institut für Experimentalphysik 1, D-44780 Bochum, Germany

J. T. Boyd, J. P. Burke, W. N. Cottingham, D. Walker

University of Bristol, Bristol BS8 1TL, United Kingdom

D. J. Asgeirsson, T. Cuhadar-Donszelmann, B. G. Fulsom, C. Hearty, N. S. Knecht, T. S. Mattison,
J. A. McKenna

University of British Columbia, Vancouver, British Columbia, Canada V6T 1Z1

A. Khan, P. Kyberd, M. Saleem, D. J. Sherwood, L. Teodorescu

Brunel University, Uxbridge, Middlesex UB8 3PH, United Kingdom

V. E. Blinov, A. D. Bukin, V. P. Druzhinin, V. B. Golubev, A. P. Onuchin, S. I. Serednyakov,
Yu. I. Skovpen, E. P. Solodov, K. Yu Todyshev

Budker Institute of Nuclear Physics, Novosibirsk 630090, Russia

D. S. Best, M. Bondioli, M. Bruinsma, M. Chao, S. Curry, I. Eschrich, D. Kirkby, A. J. Lankford, P. Lund,
M. Mandelkern, R. K. Mommsen, W. Roethel, D. P. Stoker

University of California at Irvine, Irvine, California 92697, USA

S. Abachi, C. Buchanan

University of California at Los Angeles, Los Angeles, California 90024, USA

S. D. Foulkes, J. W. Gary, O. Long, B. C. Shen, K. Wang, L. Zhang
University of California at Riverside, Riverside, California 92521, USA

H. K. Hadavand, E. J. Hill, H. P. Paar, S. Rahatlou, V. Sharma
University of California at San Diego, La Jolla, California 92093, USA

J. W. Berryhill, C. Campagnari, A. Cunha, B. Dahmes, T. M. Hong, D. Kovalskyi, J. D. Richman
University of California at Santa Barbara, Santa Barbara, California 93106, USA

T. W. Beck, A. M. Eisner, C. J. Flacco, C. A. Heusch, J. Kroseberg, W. S. Lockman, G. Nesom, T. Schalk,
B. A. Schumm, A. Seiden, P. Spradlin, D. C. Williams, M. G. Wilson
University of California at Santa Cruz, Institute for Particle Physics, Santa Cruz, California 95064, USA

J. Albert, E. Chen, A. Dvoretzkii, F. Fang, D. G. Hitlin, I. Narsky, T. Piatenko, F. C. Porter, A. Ryd,
A. Samuel
California Institute of Technology, Pasadena, California 91125, USA

G. Mancinelli, B. T. Meadows, K. Mishra, M. D. Sokoloff
University of Cincinnati, Cincinnati, Ohio 45221, USA

F. Blanc, P. C. Bloom, S. Chen, W. T. Ford, J. F. Hirschauer, A. Kreisel, M. Nagel, U. Nauenberg,
A. Olivas, W. O. Ruddick, J. G. Smith, K. A. Ulmer, S. R. Wagner, J. Zhang
University of Colorado, Boulder, Colorado 80309, USA

A. Chen, E. A. Eckhart, A. Soffer, W. H. Toki, R. J. Wilson, F. Winklmeier, Q. Zeng
Colorado State University, Fort Collins, Colorado 80523, USA

D. D. Altenburg, E. Feltresi, A. Hauke, H. Jasper, J. Merkel, A. Petzold, B. Spaan
Universität Dortmund, Institut für Physik, D-44221 Dortmund, Germany

T. Brandt, V. Klose, H. M. Lacker, W. F. Mader, R. Nogowski, J. Schubert, K. R. Schubert, R. Schwierz,
J. E. Sundermann, A. Volk
Technische Universität Dresden, Institut für Kern- und Teilchenphysik, D-01062 Dresden, Germany

D. Bernard, G. R. Bonneaud, E. Latour, Ch. Thiebaux, M. Verderi
Laboratoire Leprince-Ringuet, CNRS/IN2P3, Ecole Polytechnique, F-91128 Palaiseau, France

P. J. Clark, W. Gradl, F. Muheim, S. Playfer, A. I. Robertson, Y. Xie
University of Edinburgh, Edinburgh EH9 3JZ, United Kingdom

M. Andreotti, D. Bettoni, C. Bozzi, R. Calabrese, G. Cibinetto, E. Luppi, M. Negrini, A. Petrella,
L. Piemontese, E. Prencipe
Università di Ferrara, Dipartimento di Fisica and INFN, I-44100 Ferrara, Italy

F. Anulli, R. Baldini-Ferrolì, A. Calcaterra, R. de Sangro, G. Finocchiaro, S. Pacetti, P. Patteri,
I. M. Peruzzi,¹ M. Piccolo, M. Rama, A. Zallo
Laboratori Nazionali di Frascati dell'INFN, I-00044 Frascati, Italy

¹Also with Università di Perugia, Dipartimento di Fisica, Perugia, Italy

A. Buzzo, R. Capra, R. Contri, M. Lo Vetere, M. M. Macri, M. R. Monge, S. Passaggio, C. Patrignani,
E. Robutti, A. Santroni, S. Tosi

Università di Genova, Dipartimento di Fisica and INFN, I-16146 Genova, Italy

G. Brandenburg, K. S. Chaisanguanthum, M. Morii, J. Wu

Harvard University, Cambridge, Massachusetts 02138, USA

R. S. Dubitzky, J. Marks, S. Schenk, U. Uwer

Universität Heidelberg, Physikalisches Institut, Philosophenweg 12, D-69120 Heidelberg, Germany

D. J. Bard, W. Bhimji, D. A. Bowerman, P. D. Dauncey, U. Egede, R. L. Flack, J. A. Nash,
M. B. Nikolich, W. Panduro Vazquez

Imperial College London, London, SW7 2AZ, United Kingdom

P. K. Behera, X. Chai, M. J. Charles, U. Mallik, N. T. Meyer, V. Ziegler

University of Iowa, Iowa City, Iowa 52242, USA

J. Cochran, H. B. Crawley, L. Dong, V. Eyges, W. T. Meyer, S. Prell, E. I. Rosenberg, A. E. Rubin

Iowa State University, Ames, Iowa 50011-3160, USA

A. V. Gritsan

Johns Hopkins University, Baltimore, Maryland 21218, USA

A. G. Denig, M. Fritsch, G. Schott

Universität Karlsruhe, Institut für Experimentelle Kernphysik, D-76021 Karlsruhe, Germany

N. Arnaud, M. Davier, G. Grosdidier, A. Höcker, F. Le Diberder, V. Lepeltier, A. M. Lutz, A. Oyanguren,
S. Pruvot, S. Rodier, P. Roudeau, M. H. Schune, A. Stocchi, W. F. Wang, G. Wormser

*Laboratoire de l'Accélérateur Linéaire, IN2P3/CNRS et Université Paris-Sud 11, Centre Scientifique
d'Orsay, B.P. 34, F-91898 ORSAY Cedex, France*

C. H. Cheng, D. J. Lange, D. M. Wright

Lawrence Livermore National Laboratory, Livermore, California 94550, USA

C. A. Chavez, I. J. Forster, J. R. Fry, E. Gabathuler, R. Gamet, K. A. George, D. E. Hutchcroft,
D. J. Payne, K. C. Schofield, C. Touramanis

University of Liverpool, Liverpool L69 7ZE, United Kingdom

A. J. Bevan, F. Di Lodovico, W. Menges, R. Sacco

Queen Mary, University of London, E1 4NS, United Kingdom

G. Cowan, H. U. Flaecher, D. A. Hopkins, P. S. Jackson, T. R. McMahon, S. Ricciardi, F. Salvatore,
A. C. Wren

*University of London, Royal Holloway and Bedford New College, Egham, Surrey TW20 0EX, United
Kingdom*

D. N. Brown, C. L. Davis

University of Louisville, Louisville, Kentucky 40292, USA

J. Allison, N. R. Barlow, R. J. Barlow, Y. M. Chia, C. L. Edgar, G. D. Lafferty, M. T. Naisbit,
J. C. Williams, J. I. Yi

University of Manchester, Manchester M13 9PL, United Kingdom

C. Chen, W. D. Hulsbergen, A. Jawahery, C. K. Lae, D. A. Roberts, G. Simi

University of Maryland, College Park, Maryland 20742, USA

G. Blaylock, C. Dallapiccola, S. S. Hertzbach, X. Li, T. B. Moore, S. Saremi, H. Staengle

University of Massachusetts, Amherst, Massachusetts 01003, USA

R. Cowan, G. Sciolla, S. J. Sekula, M. Spitznagel, F. Taylor, R. K. Yamamoto

*Massachusetts Institute of Technology, Laboratory for Nuclear Science, Cambridge, Massachusetts 02139,
USA*

H. Kim, S. E. Mclachlin, P. M. Patel, S. H. Robertson

McGill University, Montréal, Québec, Canada H3A 2T8

A. Lazzaro, V. Lombardo, F. Palombo

Università di Milano, Dipartimento di Fisica and INFN, I-20133 Milano, Italy

J. M. Bauer, L. Cremaldi, V. Eschenburg, R. Godang, R. Kroeger, D. A. Sanders, D. J. Summers,
H. W. Zhao

University of Mississippi, University, Mississippi 38677, USA

S. Brunet, D. Côté, M. Simard, P. Taras, F. B. Viaud

Université de Montréal, Physique des Particules, Montréal, Québec, Canada H3C 3J7

H. Nicholson

Mount Holyoke College, South Hadley, Massachusetts 01075, USA

N. Cavallo,² G. De Nardo, F. Fabozzi,³ C. Gatto, L. Lista, D. Monorchio, P. Paolucci, D. Piccolo,
C. Sciacca

Università di Napoli Federico II, Dipartimento di Scienze Fisiche and INFN, I-80126, Napoli, Italy

M. A. Baak, G. Raven, H. L. Snoek

*NIKHEF, National Institute for Nuclear Physics and High Energy Physics, NL-1009 DB Amsterdam, The
Netherlands*

C. P. Jessop, J. M. LoSecco

University of Notre Dame, Notre Dame, Indiana 46556, USA

T. Allmendinger, G. Benelli, L. A. Corwin, K. K. Gan, K. Honscheid, D. Hufnagel, P. D. Jackson,
H. Kagan, R. Kass, A. M. Rahimi, J. J. Regensburger, R. Ter-Antonyan, Q. K. Wong

Ohio State University, Columbus, Ohio 43210, USA

N. L. Blount, J. Brau, R. Frey, O. Igonkina, J. A. Kolb, M. Lu, R. Rahmat, N. B. Sinev, D. Strom,
J. Strube, E. Torrence

University of Oregon, Eugene, Oregon 97403, USA

²Also with Università della Basilicata, Potenza, Italy

³Also with Università della Basilicata, Potenza, Italy

A. Gaz, M. Margoni, M. Morandin, A. Pompili, M. Posocco, M. Rotondo, F. Simonetto, R. Stroili, C. Voci
Università di Padova, Dipartimento di Fisica and INFN, I-35131 Padova, Italy

M. Benayoun, H. Briand, J. Chauveau, P. David, L. Del Buono, Ch. de la Vaissière, O. Hamon,
B. L. Hartfiel, M. J. J. John, Ph. Leruste, J. Malclès, J. Ocariz, L. Roos, G. Therin
*Laboratoire de Physique Nucléaire et de Hautes Energies, IN2P3/CNRS, Université Pierre et Marie
Curie-Paris6, Université Denis Diderot-Paris7, F-75252 Paris, France*

L. Gladney, J. Panetta
University of Pennsylvania, Philadelphia, Pennsylvania 19104, USA

M. Biasini, R. Covarelli
Università di Perugia, Dipartimento di Fisica and INFN, I-06100 Perugia, Italy

C. Angelini, G. Batignani, S. Bettarini, F. Bucci, G. Calderini, M. Carpinelli, R. Cenci, F. Forti,
M. A. Giorgi, A. Lusiani, G. Marchiori, M. A. Mazur, M. Morganti, N. Neri, E. Paoloni, G. Rizzo,
J. J. Walsh
Università di Pisa, Dipartimento di Fisica, Scuola Normale Superiore and INFN, I-56127 Pisa, Italy

M. Haire, D. Judd, D. E. Wagoner
Prairie View A&M University, Prairie View, Texas 77446, USA

J. Biesiada, N. Danielson, P. Elmer, Y. P. Lau, C. Lu, J. Olsen, A. J. S. Smith, A. V. Telnov
Princeton University, Princeton, New Jersey 08544, USA

F. Bellini, G. Cavoto, A. D'Orazio, D. del Re, E. Di Marco, R. Faccini, F. Ferrarotto, F. Ferroni,
M. Gaspero, L. Li Gioi, M. A. Mazzoni, S. Morganti, G. Piredda, F. Polci, F. Safai Tehrani, C. Voena
Università di Roma La Sapienza, Dipartimento di Fisica and INFN, I-00185 Roma, Italy

M. Ebert, H. Schröder, R. Waldi
Universität Rostock, D-18051 Rostock, Germany

T. Adye, N. De Groot, B. Franek, E. O. Olaiya, F. F. Wilson
Rutherford Appleton Laboratory, Chilton, Didcot, Oxon, OX11 0QX, United Kingdom

R. Aleksan, S. Emery, A. Gaidot, S. F. Ganzhur, G. Hamel de Monchenault, W. Kozanecki, M. Legendre,
G. Vasseur, Ch. Yèche, M. Zito
DSM/Dapnia, CEA/Saclay, F-91191 Gif-sur-Yvette, France

X. R. Chen, H. Liu, W. Park, M. V. Purohit, J. R. Wilson
University of South Carolina, Columbia, South Carolina 29208, USA

M. T. Allen, D. Aston, R. Bartoldus, P. Bechtle, N. Berger, R. Claus, J. P. Coleman, M. R. Convery,
M. Cristinziani, J. C. Dingfelder, J. Dorfan, G. P. Dubois-Felsmann, D. Dujmic, W. Dunwoodie,
R. C. Field, T. Glanzman, S. J. Gowdy, M. T. Graham, P. Grenier,⁴ V. Halyo, C. Hast, T. Hryn'ova,
W. R. Innes, M. H. Kelsey, P. Kim, D. W. G. S. Leith, S. Li, S. Luitz, V. Luth, H. L. Lynch,
D. B. MacFarlane, H. Marsiske, R. Messner, D. R. Muller, C. P. O'Grady, V. E. Ozcan, A. Perazzo,
M. Perl, T. Pulliam, B. N. Ratcliff, A. Roodman, A. A. Salnikov, R. H. Schindler, J. Schwiening,
A. Snyder, J. Stelzer, D. Su, M. K. Sullivan, K. Suzuki, S. K. Swain, J. M. Thompson, J. Va'vra, N. van

⁴Also at Laboratoire de Physique Corpusculaire, Clermont-Ferrand, France

Bakel, M. Weaver, A. J. R. Weinstein, W. J. Wisniewski, M. Wittgen, D. H. Wright, A. K. Yarritu, K. Yi,
C. C. Young

Stanford Linear Accelerator Center, Stanford, California 94309, USA

P. R. Burchat, A. J. Edwards, S. A. Majewski, B. A. Petersen, C. Roat, L. Wilden

Stanford University, Stanford, California 94305-4060, USA

S. Ahmed, M. S. Alam, R. Bula, J. A. Ernst, V. Jain, B. Pan, M. A. Saeed, F. R. Wappler, S. B. Zain

State University of New York, Albany, New York 12222, USA

W. Bugg, M. Krishnamurthy, S. M. Spanier

University of Tennessee, Knoxville, Tennessee 37996, USA

R. Eckmann, J. L. Ritchie, A. Satpathy, C. J. Schilling, R. F. Schwitters

University of Texas at Austin, Austin, Texas 78712, USA

J. M. Izen, X. C. Lou, S. Ye

University of Texas at Dallas, Richardson, Texas 75083, USA

F. Bianchi, F. Gallo, D. Gamba

Università di Torino, Dipartimento di Fisica Sperimentale and INFN, I-10125 Torino, Italy

M. Bomben, L. Bosisio, C. Cartaro, F. Cossutti, G. Della Ricca, S. Dittongo, L. Lanceri, L. Vitale

Università di Trieste, Dipartimento di Fisica and INFN, I-34127 Trieste, Italy

V. Azzolini, N. Lopez-March, F. Martinez-Vidal

IFIC, Universitat de Valencia-CSIC, E-46071 Valencia, Spain

Sw. Banerjee, B. Bhuyan, C. M. Brown, D. Fortin, K. Hamano, R. Kowalewski, I. M. Nugent, J. M. Roney,
R. J. Sobie

University of Victoria, Victoria, British Columbia, Canada V8W 3P6

J. J. Back, P. F. Harrison, T. E. Latham, G. B. Mohanty, M. Pappagallo

Department of Physics, University of Warwick, Coventry CV4 7AL, United Kingdom

H. R. Band, X. Chen, B. Cheng, S. Dasu, M. Datta, K. T. Flood, J. J. Hollar, P. E. Kutter, B. Mellado,
A. Mihalysi, Y. Pan, M. Pierini, R. Prepost, S. L. Wu, Z. Yu

University of Wisconsin, Madison, Wisconsin 53706, USA

H. Neal

Yale University, New Haven, Connecticut 06511, USA

1 INTRODUCTION

In 2005, *BABAR* reported the first observation of a broad structure in the $J/\psi\pi^-\pi^+$ mass spectrum produced via e^+e^- annihilation and detected in initial state radiation (ISR) events: $e^+e^- \rightarrow (J/\psi\pi^-\pi^+)\gamma$. The mass was reported to be approximately $4.26 \text{ GeV}/c^2$ and the width $\approx 90 \text{ MeV}/c^2$ if interpreted as a single resonance [1]. Subsequently, CLEO-c reported cross section measurements for $J/\psi\pi^-\pi^+$ and $J/\psi\pi^0\pi^0$ production at this mass, confirming the large production rate [2]. More recently, they have reported ISR measurements of the $J/\psi\pi^-\pi^+$ final state [3]. As discussed in refs. [1], [2], [3], and references therein, the nature of the $Y(4260)$ is not clear, so observing additional decay modes and measuring their relative rates is important for advancing our understanding of this state and its production rate.

In this paper we report measurements of $e^+e^- \rightarrow J/\psi\gamma\gamma$ cross sections using ISR events where the hard photon radiated from an initial e^+e^- collision is detected directly. Requiring that the ISR photon is detected reduces backgrounds significantly and increases the signal-to-background ratio, which we confirm with a parallel study of the benchmark signal $e^+e^- \rightarrow J/\psi\pi^-\pi^+$. In the final state $J/\psi\gamma\gamma$ we consider $J/\psi\pi^0$, $J/\psi\eta$, $\chi_{c1}\gamma$, and $\chi_{c2}\gamma$ candidates. If the $Y(4260)$ is a charmonium state, its decays might be similar to those of the $\psi(2S)$ which has relatively large branching fractions to $J/\psi\eta$, $\chi_{c1}\gamma$, and $\chi_{c2}\gamma$ [4].

The ISR cross section for a particular hadronic final state f (excluding the radiated photon) is related to the corresponding e^+e^- cross section $\sigma_f(s)$ by:

$$\frac{d\sigma_f(s, x)}{dx} = W(s, x) \cdot \sigma_f(s(1-x)) , \quad (1)$$

where $x = 2E_\gamma/\sqrt{s}$; E_γ is the energy of the ISR photon in the nominal e^+e^- center-of-mass (CM) frame; \sqrt{s} is the nominal e^+e^- CM energy; and $\sqrt{s(1-x)}$ is the effective CM energy at which the final state f is produced. The invariant mass of the hadronic final state defines the effective e^+e^- CM energy. The function $W(s, x)$ is calculated with better than 1% accuracy [5] and describes the probability density function for ISR photon emission, which occurs at all angles. For the present study we require that the hard ISR photon be detected in the electromagnetic calorimeter of the *BABAR* detector. The effective ISR luminosities at CM energies corresponding to the masses of the J/ψ , the $\psi(2S)$, and the $Y(4260)$ are $66.3 \text{ MeV}^{-1} \text{ nb}^{-1}$, $84.3 \text{ MeV}^{-1} \text{ nb}^{-1}$, and $105 \text{ MeV}^{-1} \text{ nb}^{-1}$.

2 THE *BABAR* DETECTOR AND DATASET

The data used in this analysis were collected with the *BABAR* detector at the PEP-II storage ring. The data set used here is the same data set studied in the original $Y(4260)$ analysis [1]; the integrated luminosity at and near 10.58 GeV in the e^+e^- CM is approximately 230 fb^{-1} .

Charged-particle momenta are measured in a tracking system consisting of a five-layer double-sided silicon vertex tracker (SVT) and a 40-layer central drift chamber (DCH), both situated in a 1.5-T axial magnetic field. An internally reflecting ring-imaging Cherenkov detector (DIRC) with bar radiators made of fused silica provides charged-particle identification. A CsI electromagnetic calorimeter (EMC) is used to detect and identify photons and electrons. Muons are identified in the instrumented magnetic flux return system (IFR).

Electron candidates are identified by the ratio of the shower energy deposited in the EMC to the momentum, the shower shape, the specific ionization in the DCH, and the Cherenkov angle measured by the DIRC. Muons are identified by the depth of penetration into the IFR, the IFR

cluster geometry, and the energy deposited in the EMC. Pion candidates are selected based on a likelihood calculated from the specific ionization in the DCH and SVT, and the Cherenkov angle measured in the DIRC. Photon candidates are identified with clusters in the EMC that have a shape consistent with an electromagnetic shower but without an associated charged track. A detailed description of the *BABAR* detector is available elsewhere [6].

We use an admixture of simulation packages for the final states studied. These packages use adaptations of algorithms for generating hadronic final states via initial state radiation [7], for modeling multiple soft-photons from initial-state electrons and positrons via a structure-function technique [8, 9], and for modeling photons from final-state particles [10]. We pass the generated events through a detector simulation based on GEANT4 [11], and reconstruct them in the same way as we do the data.

3 EVENT SELECTION CRITERIA

The event selection criteria used in this study, and described below, were chosen to produce very low backgrounds and to eliminate events with relatively poor mass resolution. These goals are especially important for the high-mass $J/\psi\gamma\gamma$ final state where the anticipated signal level is small. We therefore require that the ISR photon be detected directly for this analysis and do not use the much larger sample of events where the ISR photon is produced outside the EMC acceptance. To avoid bias, possible signals in the mass region above $3.85 \text{ GeV}/c^2$, were not studied until all of the selection criteria had been determined.

All charged tracks used in this analysis are required to have laboratory polar angle in the range 0.45 to 2.40 radians and are required to have at least one hit in the SVT and at least 20 hits in the DCH. Such tracks are reconstructed relatively well and are detected in a fiducial region where the particle identification is understood especially well. Candidate J/ψ mesons for the $J/\psi\gamma\gamma$ analysis are identified via their decays to $\mu^+\mu^-$. Those for the $J/\psi\pi^-\pi^+$ analysis are identified via their decays to $\mu^+\mu^-$ and e^+e^- . We require that both tracks in a dimuon candidate be identified as muons, with at least one satisfying a set of criteria which may be referred to as loose and the other satisfying a set of criteria which may be referred to as very loose. Using a sample of $\psi(2S) \rightarrow J/\psi\pi^-\pi^+$ decays produced in ISR events, we measure the muon identification efficiency for pairs to be $\approx 80\%$. Because QED production of four-lepton events is a major source of background for the $J/\psi\pi^-\pi^+$ sample, we exclude all candidates where either of the pion candidates is identified as possibly a muon or an electron. To improve the signal-to-background ratio, and because the $J/\psi \rightarrow e^+e^-$ signal has a long radiative tail and thus spans a greater mass range than does the $J/\psi \rightarrow \mu^+\mu^-$ signal, we require that both charged tracks be positively identified as electrons in selecting e^+e^- pairs. We do not measure the electron pair efficiency *per se*, but measure the $J/\psi \rightarrow e^+e^-$ efficiency relative to the $J/\psi \rightarrow \mu^+\mu^-$ efficiency using ISR $\psi(2S) \rightarrow J/\psi\pi^-\pi^+$ events.

ISR events are characterized by small missing mass, corresponding to that of the ISR photon, recoiling from the exclusive hadronic final state of interest. Experimentally, the missing mass squared, measured using the beam momentum and the momenta of the final state hadrons (including the non-ISR photons), is not exactly zero. Most importantly, higher order QED contributions to ISR production of the final state produce a very long tail at positive missing mass. In addition, the finite spread of the beam energy/momentum and the detector resolution further distort the observed values. However, the signal is predominantly produced with small recoil mass, and the signal-to-background is greatest when the observed recoil mass squared is close to zero. We exploit

this feature of the process both to select a sample of candidates with lower background rate and to improve the resolution of events selected. We require the recoil mass squared, determined from the final state particles' measured momenta and the beam particles' nominal momenta, to lie in the range -2.0 to $4.0 \text{ GeV}^2/c^4$. We also require that the missing energy, calculated in the lab, fall in the range -0.4 GeV to 1.5 GeV and that no more than 400 MeV of additional neutral energy be detected in the EMC. We then re-fit the hadronic final state particles' momenta using the nominal beam particles' momenta, the relevant track parameter error matrices, and the constraint that the recoil mass is zero. We call this the 1C fit and require its χ^2 to be less than 20. The 1C fit predicts a direction for the ISR photon. We require that the direction of the observed ISR photon candidate coincide with this predicted direction within 15 mr . In addition to reducing backgrounds, this last requirement, in the absence of any others, rejects approximately 25% of all signal candidates as a result of the higher order QED processes that contribute to the ISR cross section. In such events, the 1C fit χ^2 must also be high, so the pointing and χ^2 criteria are strongly correlated.

We select as J/ψ candidates dimuon pairs whose mass lies within $20 \text{ MeV}/c^2$ of the nominal J/ψ mass [4]. The 1C fit improves the dimuon resolution significantly, but as our charged track resolution is better than our photon resolution, this effect is less pronounced for the $J/\psi\gamma\gamma$ sample (where the J/ψ mass resolution is $\approx 12 \text{ MeV}/c^2$) than for the $J/\psi\pi^-\pi^+$ sample (where the J/ψ mass resolution is $\approx 7 \text{ MeV}/c^2$). However, as the signal-to-background (in the sample of J/ψ candidates) is worse in the $J/\psi\gamma\gamma$ sample, we use the same dimuon mass criteria for both $J/\psi\pi^-\pi^+$ and $J/\psi\gamma\gamma$ final states. For the $J/\psi\pi^-\pi^+$ channel we also select as J/ψ candidates electron pairs whose mass lies in the range $3.050 - 3.120 \text{ GeV}/c^2$. This asymmetric window around the nominal J/ψ mass is used because the signal has a long radiative tail. The specific limits of the window were chosen following studies of ISR production of $\psi(2S) \rightarrow J/\psi\pi^-\pi^+$ with $J/\psi \rightarrow e^+e^-$. We do not use $J/\psi \rightarrow e^+e^-$ candidates in this study of $J/\psi\gamma\gamma$ final states as the ISR data set used in this analysis was defined before the discovery of the $Y(4260)$, and excluded $e^+e^-\gamma\gamma\gamma$ candidates intentionally.

For the $J/\psi\gamma\gamma$ candidates accepted by the selection criteria described above, a two-constraint (2C) fit is done where the invariant mass of the lepton pair is additionally constrained to be that of the J/ψ . We then explicitly require the presence of intermediate states so that $J/\psi\gamma\gamma$ is a manifestation of $J/\psi\eta$, $J/\psi\pi^0$, $\chi_{c1}\gamma$, or $\chi_{c2}\gamma$. We require that each of the non-ISR photons has measured energy in the laboratory of at least 100 MeV and that its laboratory polar angle lies in the range 0.35 to 2.40 radians, where we understand the EMC performance well. Using momenta from the 2C fit, we require that the invariant mass of a photon pair lies in the range $0.120 - 0.150 \text{ MeV}/c^2$ to be considered as a π^0 candidate and in the range $0.52 - 0.58 \text{ MeV}/c^2$ to be considered as an η candidate. Similarly, we require that a $J/\psi\gamma$ invariant mass lies in the range $3.4906 - 3.5309 \text{ GeV}/c^2$ ($3.5363 - 3.5763 \text{ GeV}/c^2$) to be considered as a χ_{c1} (χ_{c2}) candidate. Events with such candidates are then re-fit with a third constraint requiring that the invariant mass of the corresponding combination be that of the hypothesis. When an event satisfies the nominal requirements for more than one hypothesis, the hypothesis with the best 3C χ^2 is selected as that to be used in the final analysis. Given our $\gamma\gamma$ and $J/\psi\gamma$ resolutions, these windows accept about 90% of the candidates otherwise accepted. The $J/\psi\gamma\gamma$ resolutions depend upon the mass of the final state, in particular how far above threshold it is. For the decay $Y(4260) \rightarrow J/\psi\eta$, the (simulated) resolution is $\approx 10 \text{ MeV}/c^2$. For all of the $Y(4260)$ decay modes considered, the mass resolution is negligible relative to its $\approx 90 \text{ MeV}/c^2$ width.

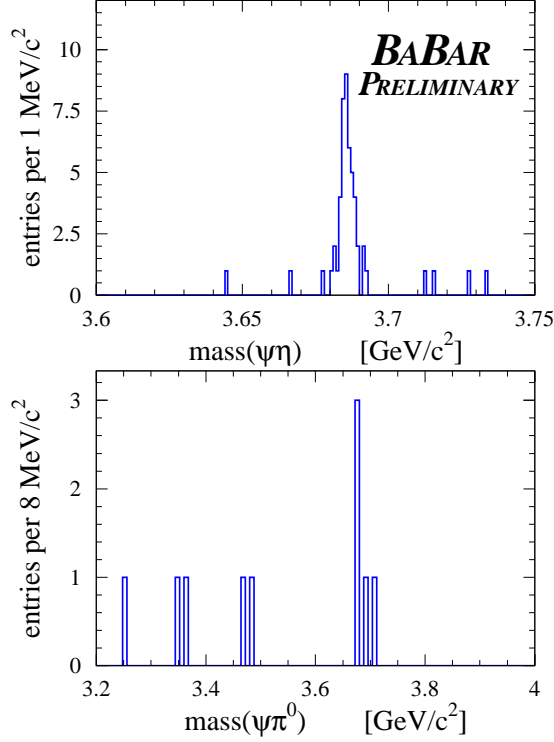


Figure 1: The upper plot shows the $J/\psi\eta$ invariant mass for $J/\psi\gamma\gamma$ candidates where $J/\psi\eta$ is the best hypothesis. The lower plot shows the $\psi\pi^0$ invariant mass for $J/\psi\gamma\gamma$ candidates where $J/\psi\pi^0$ is the best hypothesis.

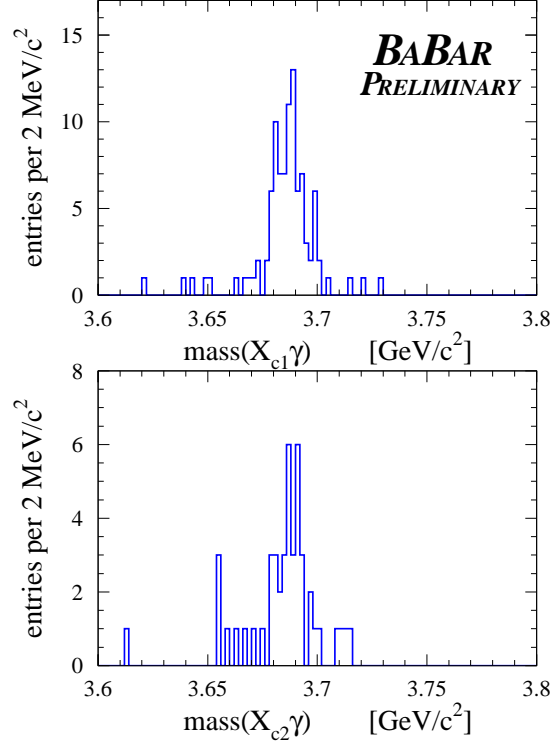


Figure 2: The upper plot shows the $\chi_{c1}\gamma$ invariant mass for $J/\psi\gamma\gamma$ candidates where $\chi_{c1}\gamma$ is the best hypothesis. The lower plot shows the $\chi_{c2}\gamma$ invariant mass for $J/\psi\gamma\gamma$ candidates where $\chi_{c2}\gamma$ is the best hypothesis.

4 MEASUREMENTS AT THE $\psi(2S)$

We initially look at signals in the $\psi(2S)$ mass region but not above $3.85 \text{ GeV}/c^2$. We also estimate background levels by looking at candidates with dimuon invariant mass in J/ψ sidebands. The $\psi(2S)$ mass region $J/\psi\gamma\gamma$ invariant mass distributions for candidates selected as $J/\psi\eta$ or $J/\psi\pi^0$ are shown in Fig. 1. The corresponding distributions for those selected as $\chi_{c1}\gamma$ or $\chi_{c2}\gamma$ are shown in Fig. 2. Note that the mass ranges of the samples differ. In particular, the $J/\psi\pi^0$ threshold is much lower, and therefore its mass resolution is much worse.

The signal levels are low in all four channels, and the background levels much lower, so we estimate the signal in each channel as the number of entries within $15 \text{ MeV}/c^2$ of the nominal $\psi(2S)$ mass. This gives 46, 4, 84, and 34 events for the $J/\psi\eta$, $J/\psi\pi^0$, $\chi_{c1}\gamma$, and $\chi_{c2}\gamma$ channels. Monte Carlo simulations indicate that the efficiencies for these channels are roughly equal (not including the branching fractions of the intermediate states). The probability that an event generated as $\chi_{c1}\gamma$ will be reconstructed as $\chi_{c2}\gamma$ or as $J/\psi\eta$ is of order 5%. The probabilities that an event generated as $J/\psi\eta$ or $J/\psi\pi^0$ will be reconstructed as $\chi_{c1}\gamma$ or $\chi_{c2}\gamma$ are of order 5% each. Altogether, the number of $\psi(2S) \rightarrow J/\psi\gamma\gamma$ signal events we observe is generally consistent with, but somewhat

higher than, the number projected from Monte Carlo studies using branching fractions (or products of branching fractions) from CLEO [12], which are generally higher than those reported by the PDG [4] in 2004.

For both samples of $J/\psi\pi^-\pi^+$ candidates accepted by the selection criteria described above, a two-constraint (2C) fit is done where the invariant mass of the lepton pair is additionally constrained to be that of the J/ψ . We observe clean $\psi(2S)$ signals with 785 candidates in the $J/\psi \rightarrow \mu^+\mu^-$ sample and 434 in the $J/\psi \rightarrow e^+e^-$ sample. In both channels the width of the peak, fit as a Gaussian, is $\approx 3 \text{ MeV}/c^2$ and the background rate is at the percent level. From the relative numbers of $\psi(2S)$ signal events in the two J/ψ decay modes, we find the combined acceptance times reconstruction efficiency to be 1.55 times that for the $J/\psi \rightarrow \mu^+\mu^-$ mode alone. We assume the same ratio holds at higher $J/\psi\pi^-\pi^+$ mass.

The integrated ISR luminosity, requiring the ISR photon to be produced in the laboratory with a polar angle in the range 0.35 to 2.40 radians, where we understand the EMC performance well, is $84.3 \text{ MeV}^{-1} \text{ nb}^{-1}$ at the mass of the $\psi(2S)$, and we estimate its fractional uncertainty to be 3%. For a narrow resonance, one may write the integrated cross section

$$\Sigma \equiv \int \sigma(E_{\text{CM}}) dE_{\text{CM}} \quad (2)$$

where σ is a resonant cross-section and is assumed to have a Breit-Wigner line shape. It is directly related to the partial decay rate to electron pairs. If the resonance has spin 1, then

$$\Sigma = \frac{6\pi^2}{m^2} \Gamma_{ee}. \quad (3)$$

Using PDG values for Γ_{ee} , m , and relevant branching fractions [4], we predict 784 $\psi(2S) \rightarrow J/\psi\pi^-\pi^+$; $J/\psi \rightarrow \mu^+\mu^-$ events with an 8% fractional error and we observe 785. In a similar exercise, we predict $\approx 17,900$ ISR $J/\psi \rightarrow \mu^+\mu^-$ events with a 4.6% fractional uncertainty and we observe $17,312 \pm 271$ events, about 97% of the predicted number. From these studies we conclude that we understand the product of ISR luminosity and $J/\psi\pi^-\pi^+$ reconstruction efficiency with no worse than 10% precision.

5 MEASUREMENTS AT HIGHER MASS

We estimate high-mass $J/\psi\gamma\gamma$ background rates due to non- J/ψ dimuon pairs in the J/ψ mass range using $\mu^+\mu^-$ background windows 75 to 175 MeV/c^2 above and below the nominal J/ψ mass. For dimuon pairs in these windows we look for η and π^0 candidates as we do for real data (except for performing the 2C fit). To create a sample of χ_C candidates, we calculate the $\mu^-\mu^+\gamma$ invariant masses, subtract the $\mu^-\mu^+$ mass, and add the J/ψ mass to compare to the χ_{c1} and χ_{c2} masses. In all four cases, we calculate an effective “ $J/\psi\gamma\gamma$ ” mass as the $\mu^-\mu^+\gamma\gamma$ mass minus the $\mu^-\mu^+$ mass plus the J/ψ mass. These background windows enclose a total of 200 MeV/c^2 while the J/ψ candidates lie within a 40 MeV/c^2 wide window, so the background is estimated by dividing the number of candidates observed by 5. This predicts between 2 and 3 background events in the $J/\psi\eta$ sample, predominantly found below 5 GeV/c^2 , and about half this amount in each of the other channels.

The high mass $J/\psi\eta$ and $J/\psi\pi^0$ data are shown in Fig. 3. The high mass $\chi_{c1}\gamma$ and $\chi_{c2}\gamma$ data are shown in Fig. 4. We see no events in the $Y(4260)$ region in the $J/\psi\eta$, $J/\psi\pi^0$, or $\chi_{c2}\gamma$ distributions, and about the total number of entries estimated as non- J/ψ $\mu^+\mu^-\gamma\gamma$. Two entries

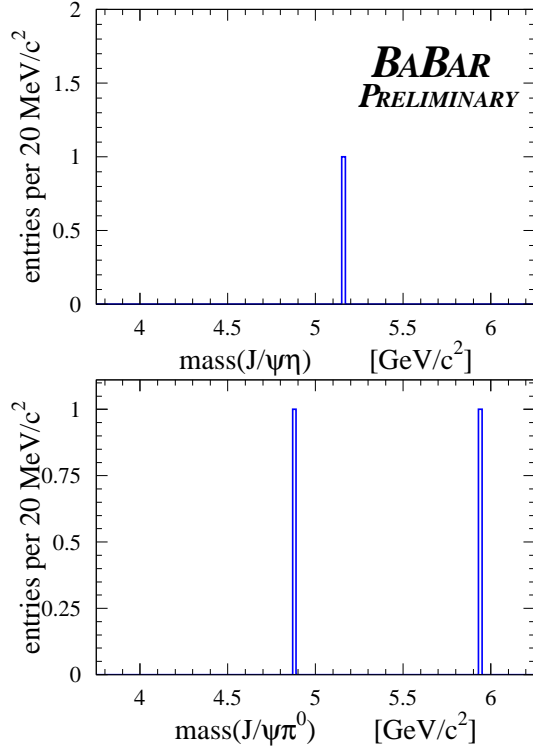


Figure 3: These are the $J/\psi \eta$ (top) and $J/\psi \pi^0$ (bottom) invariant mass distributions for candidates satisfying all final analysis criteria.

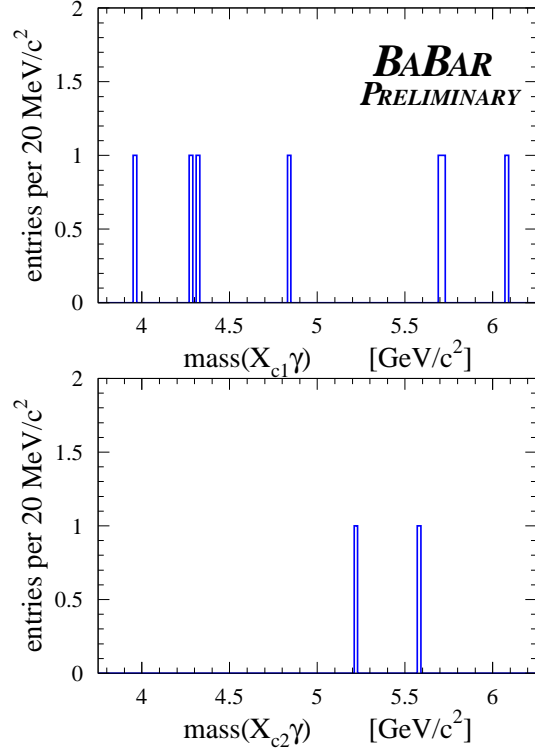


Figure 4: These are the $\chi_{c1} \gamma$ (top) and $\chi_{c2} \gamma$ (bottom) invariant mass distributions for candidates satisfying all final analysis criteria.

are observed in the $Y(4260)$ region of the $\chi_{c1} \gamma$ distribution, and six entries altogether, about two or three times the number estimated as non- $J/\psi \mu^- \mu^+ \gamma \gamma$. This leads to the question of other potential sources of background.

Excluding $J/\psi \gamma \gamma$ candidates whose invariant mass lies within $25 \text{ MeV}/c^2$ of the $\psi(2S)$, we examined the remaining $\gamma \gamma$ invariant mass distribution and separated the pairs into those from each of the four candidate categories and those in which the parent did not satisfy the criteria for any of the intermediate states. We use this last set of events to estimate how many additional background events might be observed in the $\chi_{c1} \gamma$ sample in the $Y(4260)$ mass region. The statistics of the samples are low, so a precise estimate is not possible. A reasonable estimate is that the expected background rate is between 0.5 and 1.0 additional events. Thus, we cannot exclude the possibility that both events observed are background. Neither can we exclude the possibility that they are signal. We therefore calculate the 90% confidence level upper limit assuming no background.

We calculate the 90% confidence level upper limit for the integrated cross section times branching fraction (or product of branching fractions) for each of the four channels considered using 2.3 events as the Poisson upper limit for channels where no entries are observed in the $Y(4260)$ region and 5.3 events in the case of the $\chi_{c1} \gamma$ channel where 2 entries are observed. Similarly, we use 5.3 events for calculating the upper limit for inclusive $J/\psi \gamma \gamma$ production of these states. The Monte Carlo efficiencies for the $J/\psi \eta$, $J/\psi \pi^0$, and $\chi_{c1} \gamma$ channels are 11.2%, 10.9%, and 11.9% respectively.

The efficiency for inclusive $J/\psi\gamma\gamma$ production of these states, 12.2%, is somewhat higher than the efficiencies of the exclusive final states because, in contrast to the those efficiencies, it counts as reconstructed signal also those events generated as one exclusive final state but reconstructed as another. To allow for systematic uncertainties in luminosity times reconstruction efficiency, we round off each of the precisely calculated values, increasing them by between 10% and 20%. These results are shown in Table 5. The ratio of branching fractions, with respect to $Y(4260) \rightarrow J/\psi\pi^-\pi^+$, is calculated using the cross section times branching fraction result from our original study [1]: $\Sigma \times \mathcal{B}(Y(4260) \rightarrow J/\psi\pi^-\pi^+) = (7.0 \pm 1.3 \pm 1.0) \text{ MeV nb}$.

Table 1: This table compares the integrated cross section times branching fraction results for the $Y(4260) \rightarrow J/\psi\gamma\gamma$ decay modes studied. Limits relative to $Y(4260) \rightarrow J/\psi\pi^-\pi^+$ are calculated using the cross section measured in our original study [1].

channel (X)	$\Sigma \times \mathcal{B}(X)$	$\mathcal{B}(X)/\mathcal{B}(J/\psi\pi^-\pi^+)$
$Y(4260) \rightarrow J/\psi\eta$	$< 10 \text{ MeV nb}$	< 1.4
$Y(4260) \rightarrow J/\psi\pi^0$	$< 4 \text{ MeV nb}$	< 0.6
$Y(4260) \rightarrow \chi_{c1}\gamma \rightarrow J/\psi\gamma\gamma$	$< 25 \text{ MeV nb}$	< 3.6
$Y(4260) \rightarrow \chi_{c2}\gamma \rightarrow J/\psi\gamma\gamma$	$< 18 \text{ MeV nb}$	< 2.6
$Y(4260) \rightarrow J/\psi\gamma\gamma$	$< 8 \text{ MeV nb}$	< 1.2

As it is our benchmark mode, we also study $J/\psi\pi^-\pi^+$ at high mass using selection criteria very similar to those used for $J/\psi\gamma\gamma$. We first studied expected background rates. We defined wide dilepton mass windows above and below the J/ψ mass region in both channels and used the $\ell^+\ell^-\pi^+\pi^-$ candidates in those windows as if they were $J/\psi\pi^-\pi^+$ candidates to estimate background rates. Scaling the widths of the background windows to those used for J/ψ candidates, we estimate 8 background events in the $2.5 \text{ GeV}/c^2$ range from $3.75 \text{ GeV}/c^2$ to $6.25 \text{ GeV}/c^2$, distributed more or less uniformly over that range and divided roughly equally between $J/\psi \rightarrow \mu^+\mu^-$ and $J/\psi \rightarrow e^+e^-$ candidates.

The high mass $J/\psi\pi^-\pi^+$ sample for this study is shown in Fig. 5. For comparison, the plot from our original $Y(4260)$ paper [1] is shown in Fig. 6. As anticipated, the signal level is much lower in this study and the signal-to-background ratio is much higher, primarily because here we require that the ISR photon be detected directly and not produced outside the EMC acceptance. The non- J/ψ $\mu^-\mu^+\pi^-\pi^+$ background rate in this plot, estimated from the J/ψ sidebands, is ≈ 0.064 events per $20 \text{ MeV}/c^2$ bin. It is insufficient to explain the 10 entries observed in the mass range $5.0 \text{ GeV}/c^2$ to $6.25 \text{ GeV}/c^2$, where it predicts only 4. In the window $\pm 250 \text{ MeV}/c^2$ around $4.260 \text{ GeV}/c^2$ we observe 24 events where our background prediction is 1.6. The data are consistent with a structure $90 \text{ MeV}/c^2$ in width, but the statistics are too low to draw an independent conclusion. In the original discovery of the $Y(4260)$ [1], the resonant cross section times branching ratio was measured to be $(7.0 \pm 1.3 \pm 1.0) \text{ MeV nb}$. This predicts a central value for the resonant signal level in the current analysis to be $\approx 10.5 \pm 2.5$ events. The higher event rates observed in the $Y(4260)$ mass region and at higher mass suggests the possibility of continuum $J/\psi\pi^-\pi^+$ production.

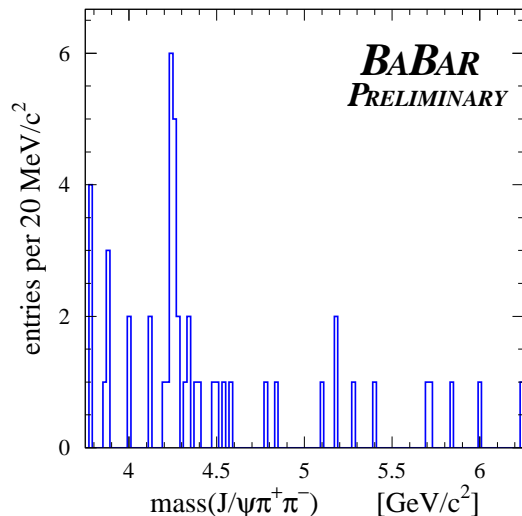


Figure 5: This is the $J/\psi \pi^- \pi^+$ invariant mass distribution for candidates satisfying all final analysis criteria.

6 SUMMARY

We observe ISR production of $\psi(2S)$ decaying into $J/\psi \eta$, $\chi_{c1} \gamma$, and $\chi_{c2} \gamma$ with summed branching fraction generally consistent with, but somewhat greater than, that reported by CLEO. We see no events in the $Y(4260)$ region in the $J/\psi \eta$, $J/\psi \pi^0$, or $\chi_{c2} \gamma$ distributions. We observe two entries in the $Y(4260)$ region of the $\chi_{c1} \gamma$ distribution, which is consistent with being either signal or background. We set 90% confidence level upper limits on the integrated cross section times branching fraction (or product of branching fractions) for each of these channels.

We observe ISR production of $J/\psi \pi^- \pi^+$ events near $4260 \text{ MeV}/c^2$ consistent with the mass and width originally reported for the $Y(4260)$ [1]. With the improved signal-to-background ratio of the analysis reported here, we observe an excess of events, both in the $Y(4260)$ mass region and at higher mass. These observations suggest continuum production of $J/\psi \pi^- \pi^+$.

7 ACKNOWLEDGMENTS

We are grateful for the extraordinary contributions of our PEP-II colleagues in achieving the excellent luminosity and machine conditions that have made this work possible. The success of this project also relies critically on the expertise and dedication of the computing organizations that support *BABAR*. The collaborating institutions wish to thank SLAC for its support and the kind hospitality extended to them. This work is supported by the US Department of Energy and National Science Foundation, the Natural Sciences and Engineering Research Council (Canada), Institute of High Energy Physics (China), the Commissariat à l’Energie Atomique and Institut National de Physique Nucléaire et de Physique des Particules (France), the Bundesministerium für Bildung und Forschung and Deutsche Forschungsgemeinschaft (Germany), the Istituto Nazionale di Fisica Nucleare (Italy), the Foundation for Fundamental Research on Matter (The Netherlands),

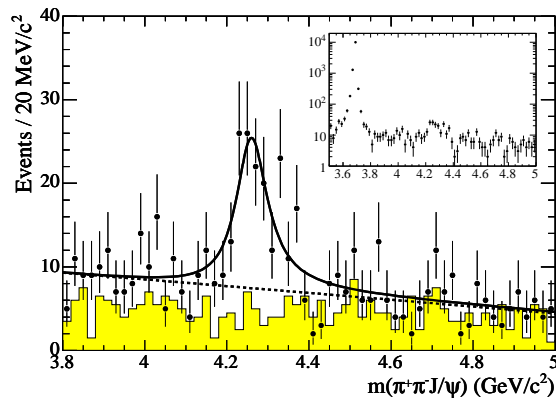


Figure 6: This is the $J/\psi \pi^- \pi^+$ invariant mass distribution presented in the original $Y(4260)$ paper [1].

the Research Council of Norway, the Ministry of Science and Technology of the Russian Federation, Ministerio de Educación y Ciencia (Spain), and the Particle Physics and Astronomy Research Council (United Kingdom). Individuals have received support from the Marie-Curie IEF program (European Union) and the A. P. Sloan Foundation.

References

- [1] The *BABAR* Collaboration, B. Aubert *et al.*, Phys. Rev. Lett. **95**, 142001 (2005).
- [2] The CLEO Collaboration, T.E. Coan *et al.*, Phys. Rev. Lett. **96**, 162001 (2006).
- [3] R. Poling, hep-ex/0606016 (2006)
- [4] Particle Data Group, S. Eidelman *et al.*, Phys. Lett. B **592**, 1 (2004).
- [5] M. Benayoun *et al.*, Mod. Phys. Lett. **A14**, 2605 (1999).
- [6] The *BABAR* Collaboration, B. Aubert *et al.*, Nucl. Instrum. Methods **A479**, 1-116 (2002).
- [7] H. Czyż and J.H. Kühn, Eur. Phys. J **C18**, 497 (2001).
- [8] A. B. Arbuzov *et al.*, J. High Energy Phys. **9710**, 001 (1997).
- [9] M. Caffo, H. Czyż, E. Remiddi, Nuovo Cim. **A110**, 515 (1997); Phys. Lett. **B327**, 369 (1994).
- [10] E. Barberio, B. van Eijk and Z. Was, Comput. Phys. Commun. **66**, 115 (1991).
- [11] GEANT4 Collaboration, S. Agostinelli *et al.*, Nucl. Instr. Methods Phys. Res., Sect. **A 506**, 250 (2003).
- [12] The CLEO Collaboration, N.E. Adam *et al.*, Phys. Rev. Lett. **94**, 232002 (2005).